

Supplementary Materials

Morphometric characterization of fibrinogen's α C regions and their role in fibrin self-assembly and molecular organization

Anna D. Protopopova, Rustem I. Litvinov, Dennis K. Galanakis, Chandrasekaran Nagaswami, Nikolay A. Barinov, Alexander R. Mukhitov, Dmitry V. Klinov, John W. Weisel

Supplementary Figures

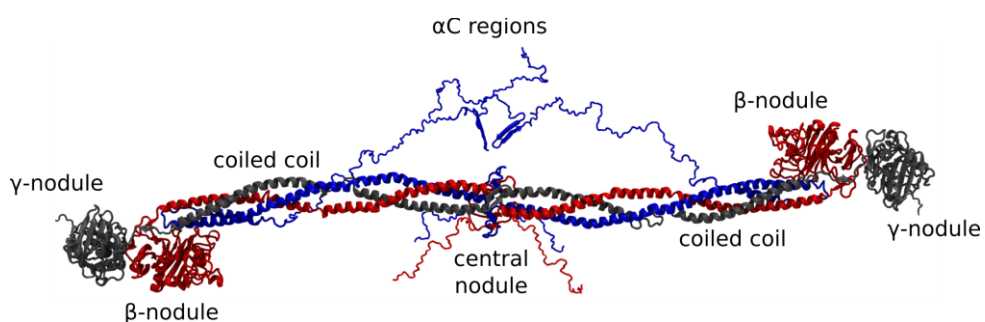


Figure S1. Structure of fibrinogen molecule. Crystal structure of the resolved parts of human Fg (PDB: 3GHG) with computationally reconstructed α C regions and the amino terminal ends of the A α and B β chains in the central nodule. A α chains are shown in blue, B β chains in red, and γ chains in black. Published with permission and thanks to Dr. Artem Zhmurov.

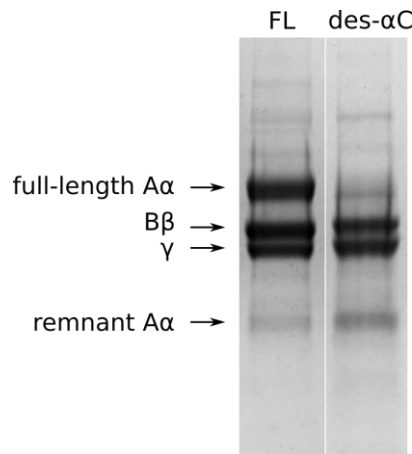


Figure S2. SDS-PAGE of fibrinogen variants. 10% SDS-PAGE in reduced conditions showing the subunit composition of a full-length Fg (FL) and a des- α C Fg variant with truncated C-terminal portion of the A α chain. Reduction of the full-length A α chain band and a corresponding increase of a remnant A α chain band indicates cleavage of the α C regions. The fractions of the full-length A α chain and its remnant (normalized by the B β chain) are estimated as 1.0 and 0.09, respectively, for the full-length Fg, and 0.11 and 0.33, respectively, for des- α C Fg. Samples were run on one gel, a white line shows where the extra lanes were spliced out. Additional analysis of the polypeptide chain composition of the different Fg subfractions can be found in.¹

Supplementary section 1. Substrate selection for AFM

In order to select the best substrate for AFM of fibrinogen and fibrin, we tested five different substrates: clean freshly cleaved mica (V-1 quality, Electron Microscopy Sciences, USA), APTES-modified mica, glow-discharged glass, and modified hydrophilized graphite. APTES-mica was prepared according to two different protocols: by vapor deposition² or by treatment of freshly cleaved mica with a diluted water solution of APTES³. Microscope glass cover slides (12-541-B Thermo Fisher Scientific, USA) were cleaned with detergent and then glow-discharged for 10 minutes. Highly oriented pyrolytic graphite (HOPG) was rendered hydrophilic with an amphiphilic graphite modifier (GM) as described in^{4,5}. Representative images of fibrinogen molecules on the surfaces used are presented in Figure S3. Two substrates were considered the most advantageous. The GM-HOPG gave the best values for the heights of globular regions (i.e. closest to the values known from the crystal structure) and had a unique ability to allow visualization of fibrinogen molecules with their α C regions exposed. The glow-discharged glass was second best in terms of

image reproducibility and it was considered a potentially good substrate for AFM imaging of fibrinogen in a buffer. Imaging on mica was poorly reproducible; modification of mica with APTES led to significant changes in flexibility of individual molecules.

The advantage of GM-HOPG over other substrates tested could be explained by multiple reasons including high surface roughness (glow-discharged glass); poor chemical stability of other surfaces (there is evidence that the surface of mica may get covered with a solid nano-layer of potassium bicarbonate under ambient conditions and in presence of water due to interaction of dissolved potassium ions with CO₂ and H₂O^{6,7}); the negative surface charge of mica and glass may also play a role in a different mode of adsorption compared to positively charged GM-HOPG.

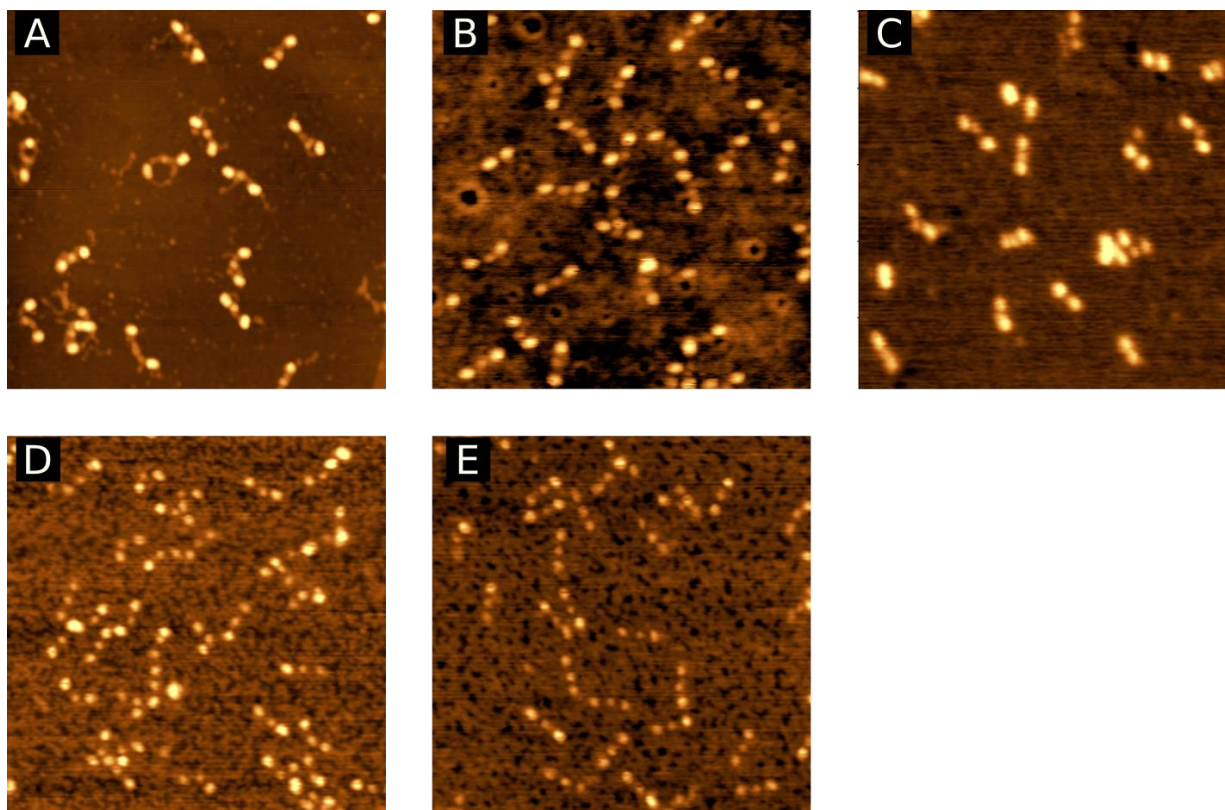


Figure S3. Representative AFM images of fibrinogen molecules adsorbed to various substrate surfaces. A: GM-HOPG; **B:** glow-discharged glass; **C:** freshly cleaved mica; **D:** mica modified with APTES by vapor depositions method; **E:** mica modified with APTES by droplet casting method. Image size 400x400 nm².

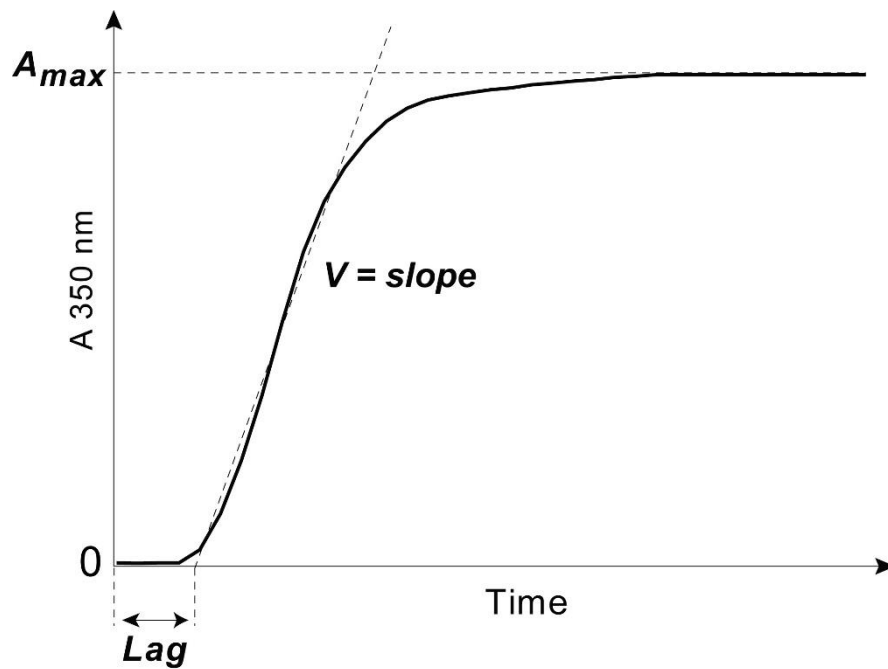


Figure S4. A typical turbidimetry curve with the following extracted parameters of fibrin formation: 1) the lag phase (Lag) or the time from initiation of reaction with thrombin until an increase of the optical density, which measures the time needed for protofibril formation; 2) the slope of the curve or the rate of polymerization (V) taken between the end of the lag phase through the linear part of the curve, which measures the velocity of lateral aggregation of protofibrils and fiber formation; 3) the maximum optical density (A_{max}) at the plateau, which reflects the amount of fibrin formed and the fibrin fiber cross-sectional area.

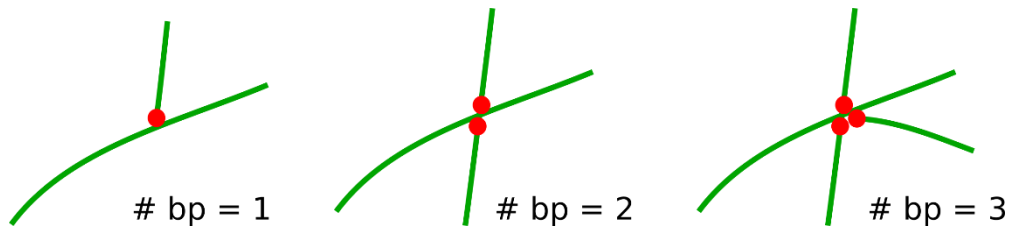


Figure S5. Number of branch points measured by the Imaris Filament Tracer in different configurations of branches.

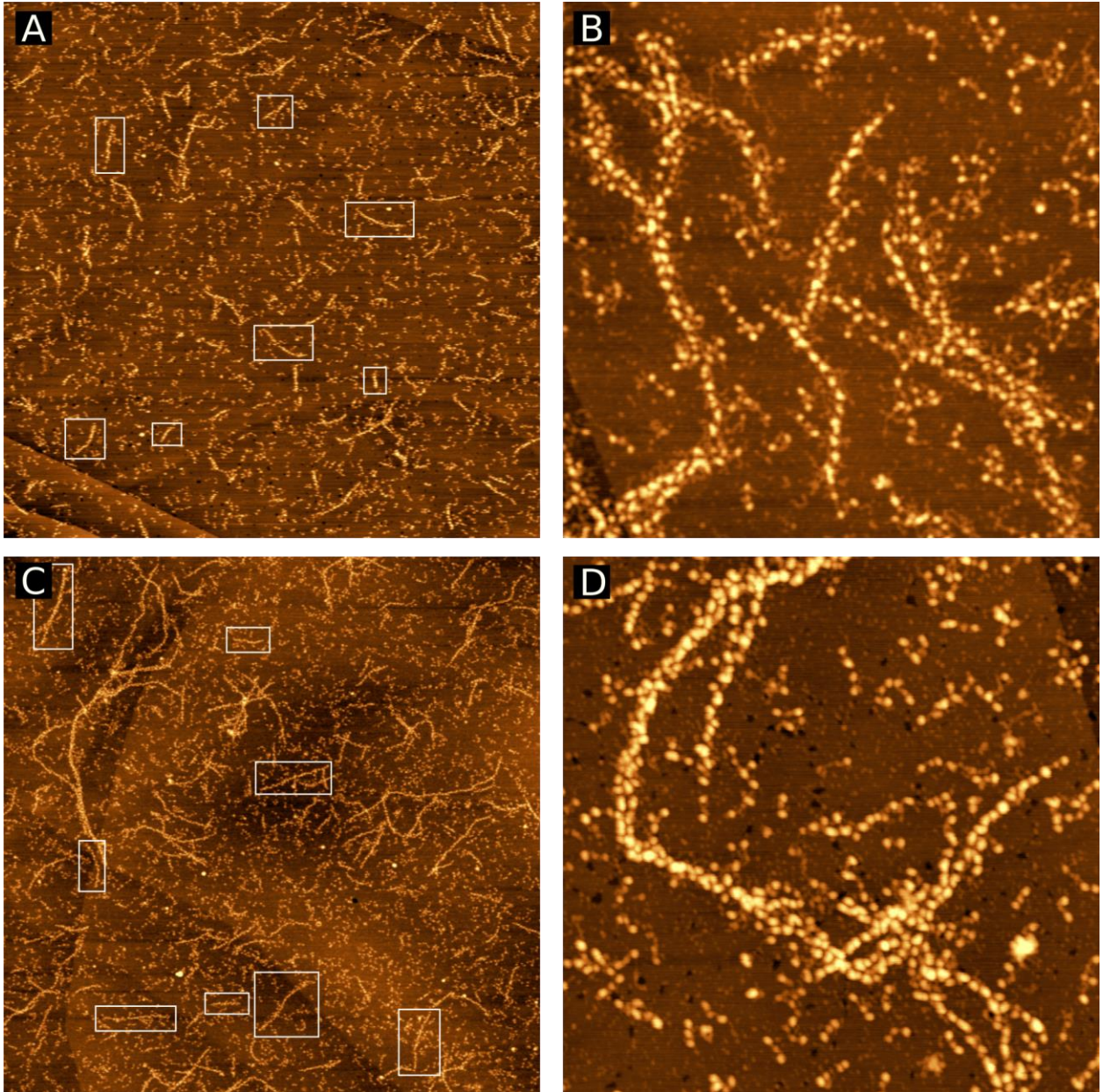


Figure S6. AFM images of intermediate products of fibrin polymerization. A and B: monomers, oligomers, and aggregating protofibrils obtained 8 minutes after the initiation of fibrin polymerization from the 0.02 mg/ml full-length Fg with 0.05 U/ml thrombin. **C and D:** monomers, oligomers, and aggregating protofibrils obtained 12 minutes after the initiation of fibrin polymerization from the 0.02 mg/ml des- α C Fg with 0.05 U/ml thrombin. Image size $4 \times 4 \mu\text{m}^2$ (A and C), $1 \times 1 \mu\text{m}^2$ (B and D). White rectangles show the examples of fibrin oligomers that were used for quantification of their length and degree of polymerization.

Supplementary Tables

Table S1. Changes in polymerization kinetics and structure of fibrin clots polymerized from Fg variants lacking α C regions compared to the full-length Fg.

	Des- α C Fg (Fg I-9) (This study)	Fragment X ⁸	Fg A α 251 ⁹	Fg A α 251 ¹⁰	Fg I-8 ¹¹
Lag period	↑	↑	↕	n/a	↑
Rate of polymerization	↓	↓	↓	n/a	↓
Max turbidity	↓	↑	↓	n/a	↓
Fiber diameter	↓	↑	n/a	↓	n/a
Branch point density	↑	n/a	n/a	↑	n/a

↑ – increase, ↓ – decrease, ↕ – no change.

Supplementary References

- 1 M. W. Mosesson, D. K. Galanakis and J. S. Finlayson, *J. Biol. Chem.*, 1974, **249**, 4656–4664.
- 2 Y. L. Lyubchenko, L. S. Shlyakhtenko and T. Ando, *Methods*, 2011, **54**, 274–283.
- 3 J. Adamcik, F. Valle, G. Witz, K. Rechendorff and G. Dietler, *Nanotechnology*, 2008, **19**, 384016.
- 4 D. Klinov, B. Dwir, E. Kapon, N. Borovok, T. Molotsky and A. Kotlyar, *Nanotechnology*, 2007, **18**, 225102.
- 5 A. D. Protopopova, N. A. Barinov, E. G. Zavyalova, A. M. Kopylov, V. I. Sergienko and D. V. Klinov, *J. Thromb. Haemost.*, 2015, **13**, 570–579.
- 6 H. K. Christenson, *J. Phys. Chem.*, 1993, **97**, 12034–12041.
- 7 V. Prokhorov, *AFM observations of single polyolefin molecules on mica and graphite*, Transworld Research Network, Kerala, India, 2012, vol. 661.
- 8 O. V. Gorkun, Y. I. Veklich, L. V. Medved', A. H. Henschen and J. W. Weisel, *Biochemistry*, 1994, **33**, 6986–6997.
- 9 O. V. Gorkun, A. H. Henschen-Edman, L. F. Ping and S. T. Lord, *Biochemistry*, 1998, **37**, 15434–15441.
- 10 J.-P. Collet, J. L. Moen, Y. I. Veklich, O. V Gorkun, S. T. Lord, G. Montalescot and J. W. Weisel, *Blood*, 2005, **106**, 3824–3830.
- 11 M. W. Mosesson, N. Alkjaersig, B. Sweet and S. Sherry, *Biochemistry*, 1967, **6**, 3279–3287.